Third International Conference on Sustainable Construction Materials and Technologies http://www.claisse.info/Proceedings.htm

Recent Advances in Carbon Fiber Reinforced Plastics

Masaki Hojo[1], Yasuo Hirose[2], Takayuki Kusaka[3] and Masaaki Nishikawa[1]

[1]*Department of Mechanical Engineering and Science, Kyoto University, Japan*
[2]*Department of Aeronautics, Kanazawa Institute of Technology, Japan*
[3]*Depatment of Mechanical Engineering, Ritsumeikan University, Japan*
[*1]*Nishikyo-ku, Kyoto 615-8540, hojo_cm@me.kyoto-u.ac.jp, nishikawa@me.kyoto-u.ac.jp*
[*2]*Nonoichi, Ishikawa 921-8501, hirose_yasuo@neptune.kanazawa-it.ac.jp*
[*3]*Kusatsu, Shiga 525-8577, kusaka@se.ritsumei.ac.jp*

ABSTRACT

Carbon fiber reinforced plastics (CFRPs) have superior specific strength and stiffness. Their application is quite active in the aerospace area where the lightweight structures are critical. This article briefly review key characteristics and current status of advanced composite materials, and further research trends from the viewpoints of structural and material developments. First one is the development of crack arrester for sandwich structures, which are expected to realize the full potential capability of composite materials. The second one is the novel through-the-thickness reinforcement technique for laminates, which is expected to improve the weakest point of common laminated structures of CFRP.

Keywords. Composite materials, Delamination, Sandwich structure, Through-thickness reinforcement, Fracture mechanics

INTRODUCTION

The last quarter of 20th century to today is probably the most significant periods for composite materials because their structures are replacing metal structures for most of the aircraft applications. Following the secondary structures in the early 1980s, the carbon fiber reinforced plastic (CFRP) structures were applied as the primary structures of vertical tail in 1985 as a representative of structures made of advanced composite materials. The newest generations of commercial airplanes have all-composite main wings and fuselages, resulting in outstanding fuel efficiency and contributing to future sustainable society. The start of commercial service of the Boeing 787 (Fig. 1) in 2011, and the expected maiden flight of Airbus A350XWB in 2013 promise that CFRPs become common structural materials for commercial aircraft. The weight ratio of composite materials for these aircraft is about 50% (Roeseler et al, 2007), corresponding volume ratio of about 70% by a simple conversion equation.

Advanced composite materials used in aerospace engineering are composed of high-performance fibers like carbon and thermoset or thermoplastic matrices like epoxy, PPS, PEEK, etc. Representative carbon fiber which is used for structures is PAN based carbon fiber, and this was invented by Shindo in 1959 in Japan (Shindo, 1959, 1961). About 2/3 of

Figure 1. Boeing 787 operated by ANA. Itami Airport, 11 March, 2012.

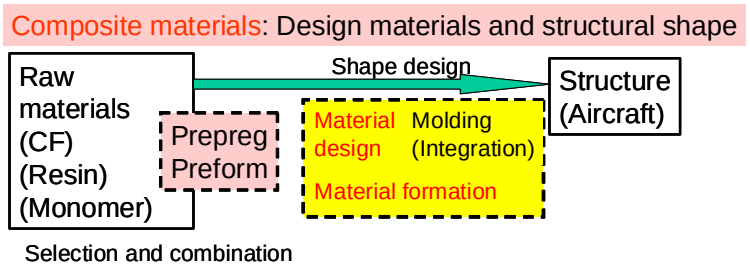

Figure 2. Simultaneous design and manufacturing process for materials and structures in composite materials.

the world's carbon fiber market was contributed by Japanese industries at present (Toray, Teijin-Thoho and Mitsubishi Rayon).

CFRPs have much higher specific strength and stiffness than any other structural materials, and this essential reason are utilized in the application of the aerospace area where the lightweight is critical. Another important feature for composite materials is the close relation between materials and structures (Figure 2). For structures made of conventional materials, there is a clear difference in functions between steel industries (material design and its manufacturing processes) and automobile and civil industries (structural design and manufacturing processes of products). On the other hand, aircraft structures are designed and processed simultaneously in aircraft industries. Here, composite structures are directly manufactured from raw constituents of composite materials like fibers and resins. Material formation and structural manufacturing take place at the same time. This also means that the changes in structural design will bring further superior capability of composite structures.

A common way to produce composite structures is to lay up thin resin impregnated and aligned fiber layers (so called prepreg) with optimized fiber direction in each layers using an autoclave. The composite laminated structures are reinforced by fibers only inside the plane, and there is no reinforcement in through-the-thickness direction. Although 30 years have passed since the importance of the interlaminar fracture was recognized (O'Brien, 1982), interlaminar strength is still one of the design limiting factors in composite laminated structures (Paul, 2002). Improving interlaminar fracture toughness is an eternal topic in composite laminated structures. Moreover, special interlayer-toughened type laminates are used as the fuselage and wings of aircraft to overcome these difficulties (Hojo et al., 2006).

Current topics are to replace metal to composite for the next development projects of commercial aircraft. In these applications, further improvements in materials and structures are requested. In the present paper, two examples are introduced from the viewpoints of structures and materials. First one is the development of crack arrester for sandwich structures. The present generation composite aircraft, Boeing 787 and Airbus A350XWB mainly use the conventional skin-stringer concepts by replacing only materials from metals to CFRPs. Then, weight and cost reduction are limited. Foam core sandwich panel structures are a promising concept for integral structures because these structures realize the full potential of composite materials. In these sandwich structures, impact damage causes delamination between surface skins and foam core. Then, the suppression of delamination is the critical issue to improve the damage tolerance capability of this concept. We have been proposing simple interfacial crack suppression methods for foam core sandwich panels by installing a material with higher stiffness on the crack path as the "crack arrester". The validity of this arrester concept is introduced in the first part (Hirose et al., 2009, 2012).

In the second part, a novel through-the-thickness reinforcement technique for CFRP laminates is introduced. Here, in-plane yarns are entangles with each other in thickness direction. This method can improve interlaminar strength both under static and fatigue loadings inexpensively together with liquid resin molding (Kusaka et al., 2012, Hojo et al., 2010).

CRACK ARRESTER FOR SUNDWICH PANEL

Materials and Specimens. Two types of crack arresters are proposed as shown in Fig. 3. The first one is a basic type arrester with semi-cylindrical shape. Here, CFRP was placed between the surface skin and form core. The second one is a splice-type arrester. In the form core sandwich panels, the core material is often divided into several pieces to match the required counters and part size. Here, the pieces are spliced with each other with a tapered butt joint with epoxy adhesive. Thin CFRP layers are inserted at the splice portion to act as the arrester.

The specimen is made of CF/toughened epoxy (UT500/#135) surface skin and a PMI (Polymethacrylimide, Rohacell WF110) foam core. The surface skin consists of 12K twill weave fabric. Its ply orientation for the semi-cylindrical type arrester is [(+45,-45)/(0,90)/(0,90)/ (+45,-45)]s, and that for the splice type arrester is [(+45,-45)/(0,90)]s. The

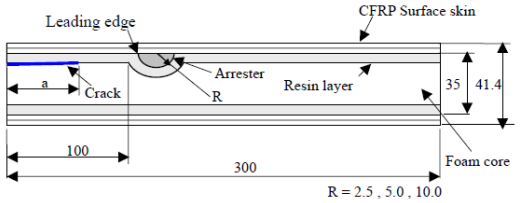

(a) Semi-cylindrical type arrester

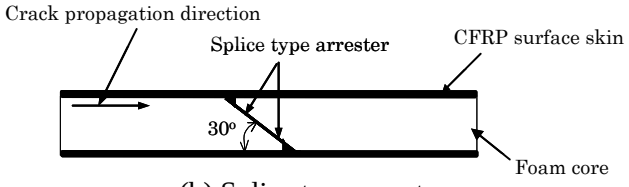

(b) Splice type arrester

Figure 3. Two types of crack arrester for sandwich panels

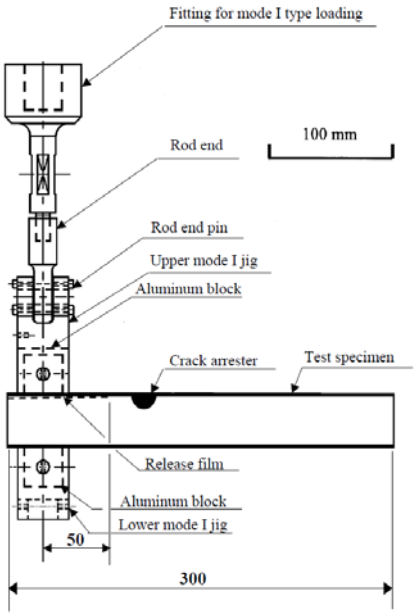

Figure 4. Specimen and loading apparatus for semi-cylindrical arrester

surface skin and foam core were placed together and were joined using resin squeezed from the CFRP prepreg during molding. For the case of the semi-cylindrical type arrester, the same CFRP with unidirectional fiber (90 direction) was used for the material of the crack arrester. For the case of the splice type arrester, one (+45,-45) ply fabric covered each foam core, and two (0,90) plies were inserted between the tapered cores. Then, total of four plies forms the splice-type arrester. Fillers with unidirectional CFRP (90 direction) were installed at the trimmed edge of the corners. A Kapton film with 12.5 μm thickness was inserted between the surface skin the foam core as a starter crack for both specimens. This film was coated with a release agent.

Analytical and Experimental Procedure. Two dimensional FE analyses were carried out to calculate the energy release rates and to evaluate the effect of the crack arrester. The energy release rates at the crack tip with and without the crack arrester were calculated using the crack closure integral.

Fig. 4 shows a schematic diagram of the specimen and the loading apparatus for the semi-cylindrical type arrester. A similar loading apparatus was used for the splice type arrester. Tests were carried out in a servo-hydraulic testing machine (Instron 8500) with a 5 kN load cell. The test speed was 2.0 mm/min. Mode I type opening loading was applied to the specimen. The location of the crack tip was measured using a traveling microscope at a magnification of 50 times.

Results and Discussion (1) Semi-cylindrical Type Arrester. Solid squares in Fig. 5 show the analytical results of the relation between the normalized energy release rate and the distance from the edge of the arrester. Here, the normalized energy release rate was defined as the ratio of the energy release rate for the specimens with arrester (G_A) to that without arrester (G_0) under the same load and the crack length. This figure clearly indicates the arrester effect where the normalized energy release rate decreased to 0.1 when the crack tip is located 0.9 mm from the arrester edge. Open circles in Fig. 5 indicate the results with a

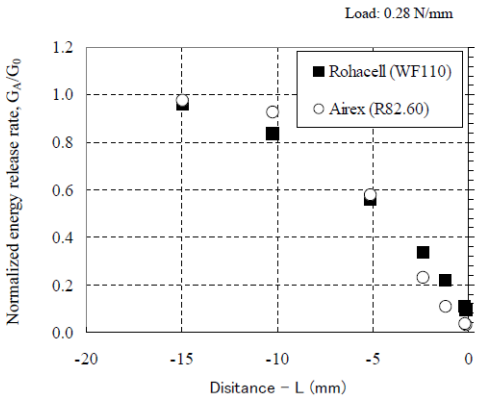

Figure 5. Relationship between normalized energy release rate and distance of crack tip from arrester edge for semi-cylindrical arrester (surface skin: 8 plies)

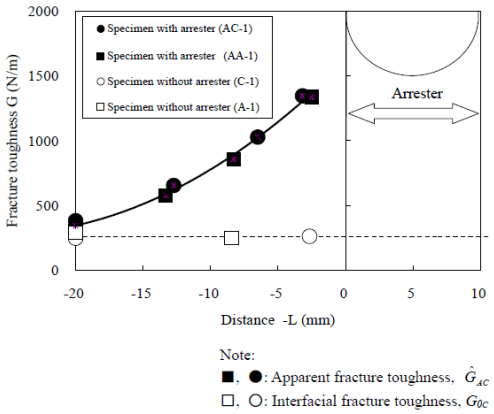

Figure 6. Relationship between fracture toughness and distance of crack tip from arrester edge for tests with and without arrester (surface skin: 8 plies)

different foam core material, Airex R82.60 (PEI, Polyetherimide). Since the stiffness of the arrester is 50 to 300 times greater than those of Rohacell WF110 and Airex R82.60, the effect of the foam core modulus is rather small.

Results of the fracture toughness tests indicated that the crack propagated between the resin-impregnated layer of the foam core and the original foam core. The thickness of this resin-impregnated layer was about 0.3 to 0.4 mm. Fig. 6 indicates the corresponding fracture toughness values. Here, while the exact toughness was plotted for the specimen without arrester, the apparent fracture toughness was plotted for the specimen with arrester. The apparent fracture toughness was calculated using the critical experimental load with arrester and the FEM model without arrester in order to indicate the arrester effect. This figure indicates that the effect of this semi-cylindrical type arrester is about five times.

We also applied this semi-cylindrical type arrester under fatigue loading. The experimental results showed clear effects of the arrester against fatigue delamination growth. It is interesting to note that the arrester effect under fatigue loading was almost the same as that under static loading.

Results and Discussion (2) Splice Type Arrester. Solid diamonds in Fig. 7 show the analytical results of the relation between the normalized energy release rate and the distance from the edge of the splice type arrester. The results of the semi-cylindrical type arrester are reproduced as open marks in this figure. It is interesting to note that the effect of the splice type arrester is larger than that of the semi-cylindrical type arrester specially when filler is introduced at the trimmed edge of the corners. Fig. 8 indicates the fracture toughness values for the specimen with and without arrester. Here, while the exact toughness was plotted for the specimen without arrester, the apparent fracture toughness was plotted for the specimen with arrester. This figure clearly indicates that the effect of the splice type arrester is about 13 times. This effect is much higher than that for the basic type arrester. This tendency also agrees with the analytical results in Fig.8. Then, this splice type arrester is recommended for the structures with higher load.

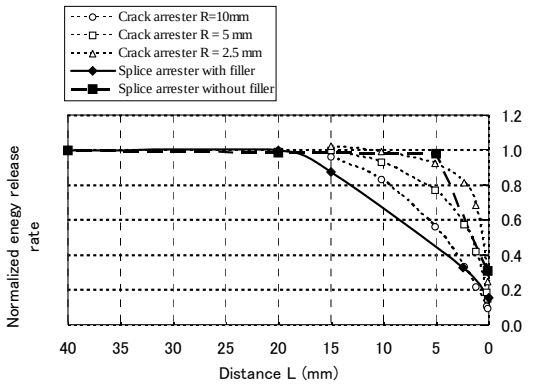

Figure 7. Relationship between normalized energy release rate and distance of crack tip from arrester edge for splice type arrester (surface skin: 4 plies)

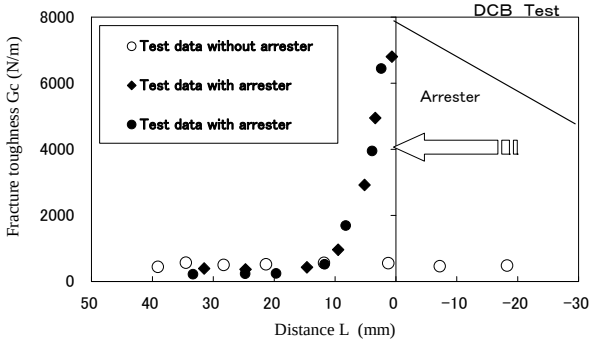

Figure 8. Relationship between fracture toughness and distance of crack tip from arrester edge for tests with and without arrester (surface skin: 4 plies)

THROUGH-THE-THICKNESS REINFORCEMENT WITH ZANCHOR

Materials and Specimens. Figure 9 shows schematic of Zanchor processing. In-plane yarns are entangled with each other using special needles. CF/epoxy cross-ply laminates of [0˚/90˚/90˚/0˚]s in a stacking sequence were molded with a Zanchor-reinforced high-strength intermediate-modulus carbon fiber dry fabric with modified epoxy using resin film infusion (RFI). Three different levels of Zanchor reinforcement (Zanchor 1, Zanchor 2 and Zanchor

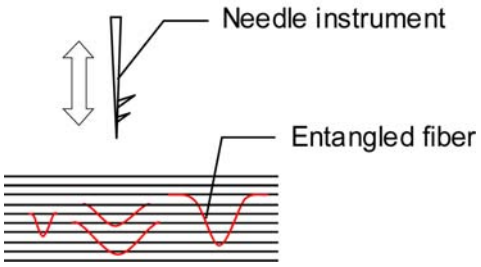

Figure 10. Schematic of through-the-thickness reinforcement by Zanchor

4) were used. Here Zanchor density is the non-dimensional parameter proportional to the number of Zanchor reinforcements per unit area. Base laminates without Zanchor reinforcement (Zanchor 0) were also fabricated for comparison. The nominal thickness of the laminates was 2.4 mm. The fiber volume fractions were about 60%. The detailed fiber microstructures of the Zanchor-reinforced laminates are given in (Hojo et al., 2010). Unidirectional CF/epoxy laminates were bonded on both surfaces of the specimens to prevent bending failure.

Double cantilever beam (DCB) specimens (width B=10 mm, length=170 mm) were used for tests under mode I loading. The initial crack length was 40 mm. Special loading apparatus with universal joints were used for the tests. Mode I precracks of less than 5 mm length were introduced into the specimens.

Fracture Toughness Test Methods. The energy release rate for DCB specimens was calculated using the modified compliance calibration method. The tests were carried out in a computer-controlled servohydraulic testing system (Shimadzu 4880, 9.8kN). A load cell of 490 N capacity was attached to the testing machine. The crosshead speed was controlled to be 0.5 mm/min. All tests were carried out at room temperature in laboratory air.

Results and Discussion. Fig. 11 shows the relationship between the mode I fracture toughness and the increment of crack length (R-curves) for all laminates (Zanchors 0 to 4). In this figure, the data points are the results of three specimens averaged at an interval of 5 mm. The propagation values of the fracture toughness, G_{IR}, for Zanchor 0 gradually increased with the increment of the crack length, Δa, from the initial value, G_{Ic}, at Δa=0mm. The G_{IR} for Zanchor 1 to 4 rapidly increased during the early stage of crack extension (Δa <15mm), and increased gradually when Δa was larger than 15 mm. The initial values, G_{Ic}, for Zanchor 0 to 4 laminates are 110, 220, 230 and 240 J/m^2, respectively. The selected representative fracture toughness values of G_{IR} at Δa=10mm, $G_{I,10mm}$, for Zanchor 0 to 4 laminates are 230, 540, 820, and 2000 J/m^2, respectively. For conventional toughened CFRP laminates, G_{IR} values are only 1.2 to 1.4 times larger than G_{Ic}. Those for ionomer toughened CFRP laminates are 1.4 to 2.3 times larger than G_{Ic}. The present results (2.5 to 8.3 times larger) indicate that the increase in the fracture toughness from the initial values is much larger than already reported laminates. This fact also suggests the difference in the reinforcing mechanism.

The relative increase in the fracture toughness from the base Zanchor 0 laminates was expressed by $\Delta G_{IRi}=G_{IRi}-G_{IR0}$ (i=1,2,4). Here, G_{IRi} and G_{IR0} are the fracture toughness of Zanchor i and Zanchor 0 laminates at each increment of crack length in Fig. 11. Since the Zanchor density is proportional to the number of Zanchor laminates, i, ΔG_{IRi} is normalized by i to investigate the mechanism of Zanchor reinforcement.

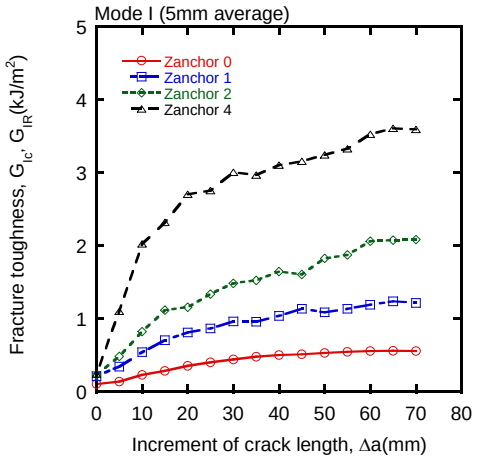

Figure 11. Relationship between fracture toughness and increment of crack length

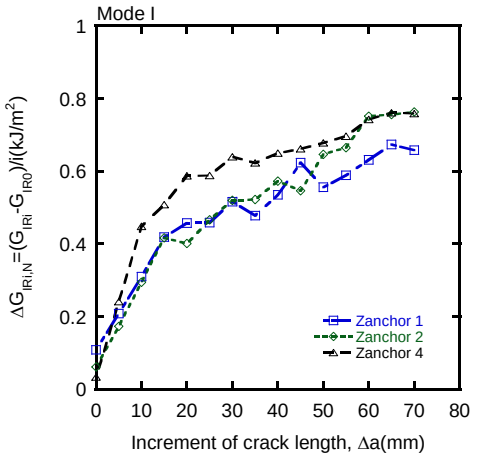

Figure 12. Relationship between normalized relative increase in fracture toughness from Zanchor 0 and increment of crack length

$$\Delta G_{IRi,N}=\Delta G_{IRi}/i=(G_{IRi}-G_{IR0})/i \quad (i=1,2,4). \qquad (1)$$

Fig.12 shows the relationship between the normalized relative increase in fracture toughness from Zanchor 0 laminates, $\Delta G_{IRi,N}$, and the increment of crack length for all laminates. This figure clearly indicates that the in-crease in the fracture toughness from the base laminates is linearly correlated to the Zanchor density.

Microscopic observations suggest that a large amount of fiber bridging induced by Zanchor process is the key factor for the dramatic increase of the fracture toughness from the base laminates under mode I loading. Fatigue tests were also carried out for Zanchor 0 and 2 laminates.

SUMMARRY

Delamination is still one of the key factors to assure the structural integrity of composite structures. From the viewpoint of structural design, two types of the crack arrester were

introduced as simple methods to suppress delamination for sandwich structures, which are expected to fully utilize the potential of composite materials. One is a semi-cylindrical type arrester and the other is a splice type arrester. Under static mode I loading, the suppression effect evaluated by the energy release rate is 5 times for the semi-cylindrical type arrester and 13 times for the splice type arrester.

From the viewpoint of material design, laminates with Zanchor was introduced as an example of the through-the-thickness reinforcement. The fracture toughness dramatically increased with Zanchor process, and this increase was roughly proportional to the Zanchor density. The obtained fracture toughness levels were one of the highest among existing toughened material systems.

REFERENCES

Hirose, Y., Matsuda, H., Matubara, G., Inamura, F., and Hojo, M. (2009). "Evaluation of new crack suppression method for foam core sandwich panel via fracture toughness tests and analyses under mode-I type loading.", *Journal of Sandwich Structures and Materials*, 11, 451-470.

Hirose, Y., Matsuda, H. Matsubara, G., Hojo, M. and Inamura, F. (2012). "Proposal of the concept of splice-type arrester for foam core sandwich panels.", *Composites: Part A*, 43 1318–1325.

Hojo, M., Matsuda, S., Tanaka, M., Ochiai, S., and Murakami, A. (2006). "Mode I delamination fatigue properties of interlayer-toughened CF/epoxy laminates." *Composites Science and Technology*, 66, 665–75.

Hojo, M., Nakashima, K., Kusaka, T., Tanaka, M., Adachi, T., Fukuoka, T., and Ishibashi, M. (2010). "Mode I fatigue delamination of Zanchor-reinforced CF/epoxy laminates.", *International Journal of Fatigue*, 32, 37-45.

Kusaka, T., Watanabe, K., Hojo, M., Fukuoka, T., and Ishibashi, M. (2012). "Fracture behaviour and toughening mechanism in Zanchor reinforced composites under mode I loading." *Engineering Fracture Mechanics*, 96, 433-446.

O'Brien T.K. (1982) "Characterization of delamination onset and growth in a composite laminate." In: Reifsnider KL, editor. *Damage in composite materials*, ASTM STP 775; 140–67.

Paul K., Kelly L., Venkayya V., Hess T. (2002) "Evolution of US military aircraft structures technology." *J Aircraft*, 39, 18–29.

Roeseler W.G., Sarh B., and Kismarton M.U. (2007). "Composite structures: the first 100 years." *Proc. of 16th international conference on composite materials, ICCM-16*, CD-ROM, MoAM1-01:1–10.

Shindo, A. (1959). Japan Patent Publication No. (1962)4405, Patent Application No. (1959)28287

Shindo, A. (1961). "Studies on graphite fibre", *Reports of the Government Industrial Research Institute, Osaka*, No. 317, 1-52